

## Supplementary Information for:

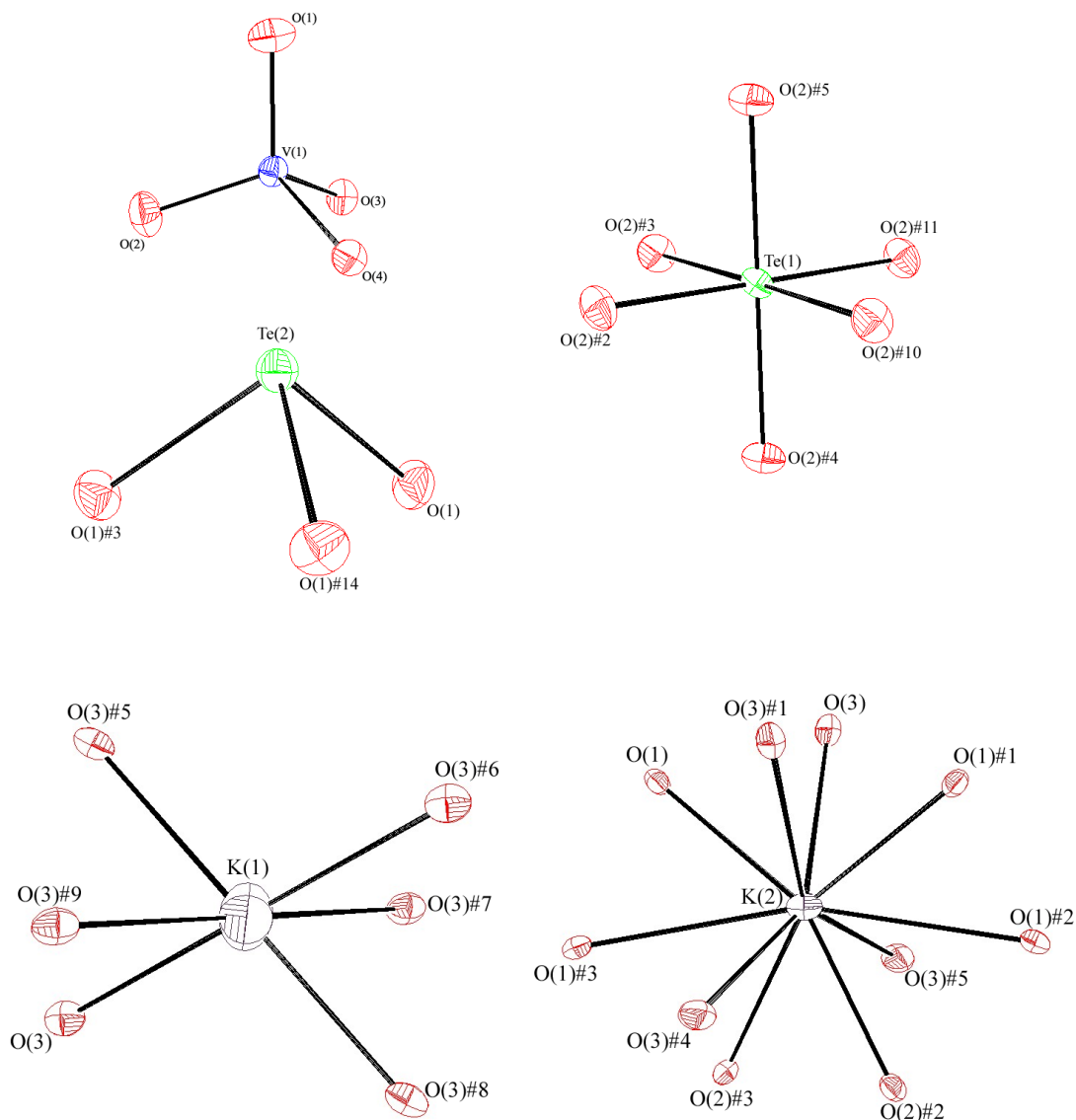
# Synthesis and Structure of $A_4V_6[Te_2^{4+}Te^{6+}]O_{24}$ ( $A = K, Rb$ ) — Two New Quaternary Mixed-Valent Tellurium Oxides

Tianxiang Zhu<sup>a</sup>, Jingui Qin<sup>\*a</sup> and P. Shiv Halasyamani<sup>b</sup>

<sup>a</sup>Department of Chemistry, Hubei Key Lab on Organic and Polymeric Opto-electronic Materials, Wuhan University, Wuhan 430072, China, and <sup>b</sup> Department of Chemistry, 136 Fleming Building, University of Houston, TX 77204-5003, USA

- S1. ORTEP (50% probability level ellipsoids) diagrams for the  $VO_4$ ,  $TeO_3$  and  $TeO_6$  polyhedra and the  $KO_6$ ,  $KO_{10}$  polyhedra for  $K_4V_6Te_3O_{24}$
- S2. ORTEP (50% probability level ellipsoids) diagrams for the  $VO_4$ ,  $TeO_3$  and  $TeO_6$  polyhedra and the  $RbO_6$ ,  $RbO_{10}$  polyhedra for  $Rb_4V_6Te_3O_{24}$
- S3. Experimental and calculated powder X-ray diffraction patterns for  $K_4V_6Te_3O_{24}$
- S4. Experimental and calculated powder X-ray diffraction patterns for  $Rb_4V_6Te_3O_{24}$
- S5. Thermogravimetric plots for  $K_4V_6Te_3O_{24}$  and  $Rb_4V_6Te_3O_{24}$
- S6. Bond strain index (BSI), global instability index (GII) and bond valence data for  $K_4Te_3V_6O_{24}$  and  $Rb_4Te_3V_6O_{24}$

S1. ORTEP (50% probability level ellipsoids) diagrams for the  $\text{VO}_4$ ,  $\text{TeO}_3$  and  $\text{TeO}_6$  polyhedra and the  $\text{KO}_6$ ,  $\text{KO}_{10}$  polyhedra for  $\text{K}_4\text{V}_6\text{Te}_3\text{O}_{24}$



Symmetry transformations used to generate equivalent atoms:

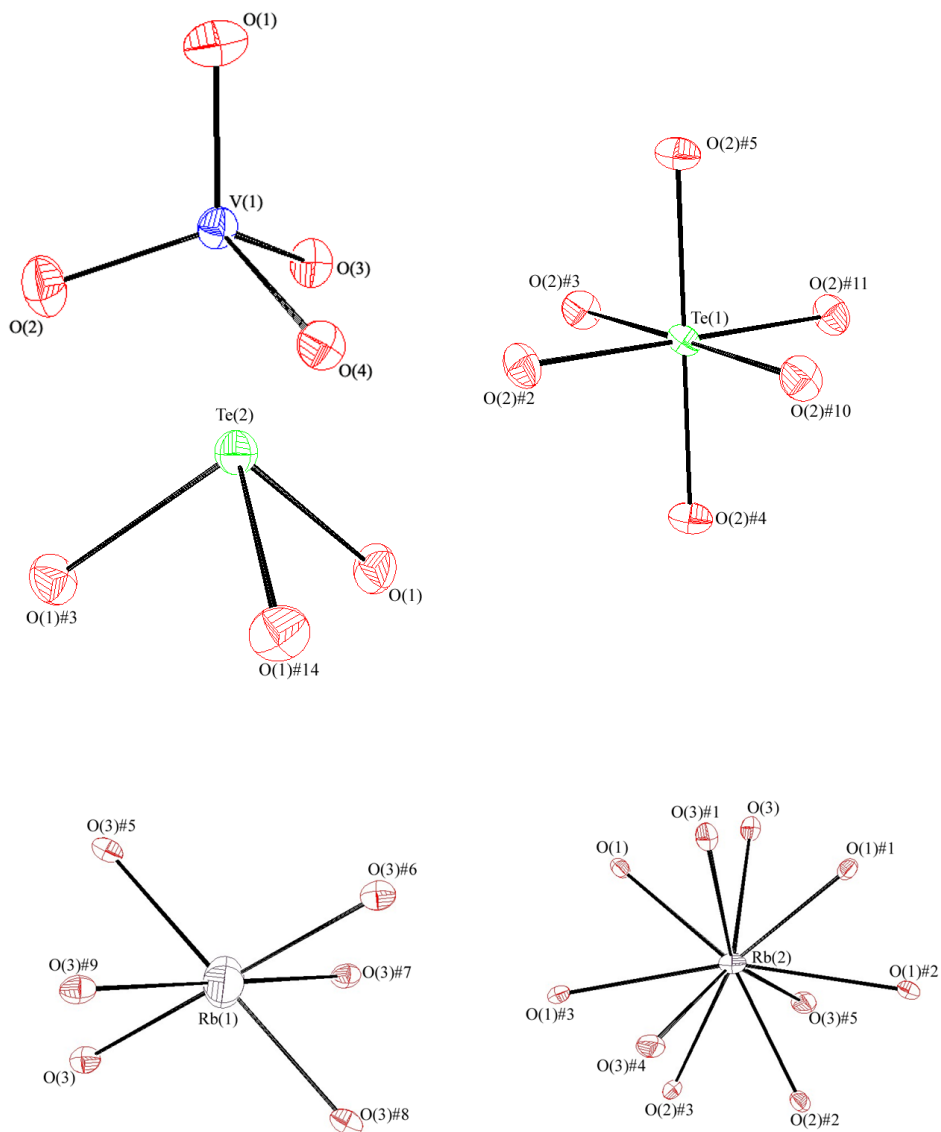
#1  $x-y+1/3, -y+2/3, -z+1/6$  #2  $y+1/3, x-4/3, -z+1/6$  #3  $-x+y+2, -x+2, z$

#4  $-x+7/3, -x+y+5/3, -z+1/6$  #5  $-y+1, x-y-1, z$  #6  $-x+2, -y, -z$  #7  $-x+y+2, -x+1, z$

#8  $y+1, -x+y+1, -z$  #9  $x-y, x-1, -z$  #10  $x-y-2/3, -y+2/3, -z+1/6$  #11  $x-1, y, z$

#12  $-x+y+1, -x+1, z$  #13  $-y+1, x-y, z$  #14  $-y+2, x-y, z$  #15  $x+1, y, z$

S2. ORTEP (50% probability level ellipsoids) diagrams for the VO<sub>4</sub>, TeO<sub>3</sub> and TeO<sub>6</sub> polyhedra and the RbO<sub>6</sub>, RbO<sub>10</sub> polyhedra for Rb<sub>4</sub>V<sub>6</sub>Te<sub>3</sub>O<sub>24</sub>



Symmetry transformations used to generate equivalent atoms:

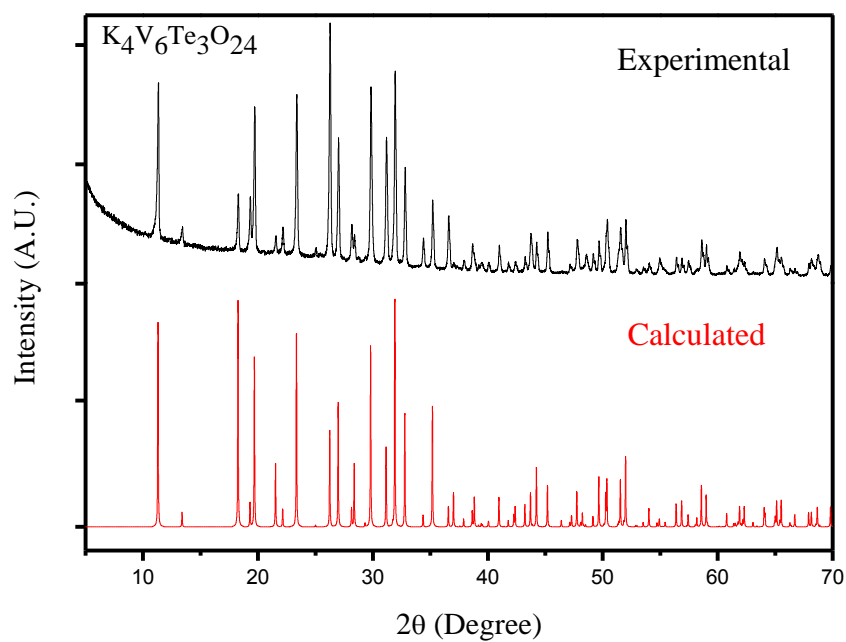
#1  $x-y+1/3, -y+2/3, -z+1/6$  #2  $y+1/3, x-4/3, -z+1/6$  #3  $-x+y+2, -x+2, z$

#4  $-x+7/3, -x+y+5/3, -z+1/6$  #5  $-y+1, x-y-1, z$  #6  $-x+2, -y, -z$  #7  $-x+y+2, -x+1, z$

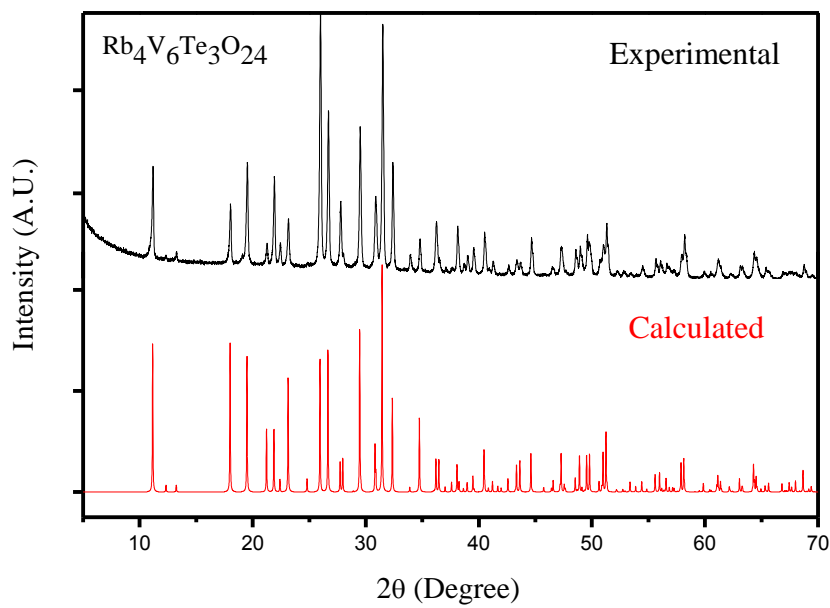
#8  $y+1, -x+y+1, -z$  #9  $x-y, x-1, -z$  #10  $x-y-2/3, -y+2/3, -z+1/6$  #11  $x-1, y, z$

#12  $-x+y+1, -x+1, z$  #13  $-y+1, x-y, z$  #14  $-y+2, x-y, z$  #15  $x+1, y, z$

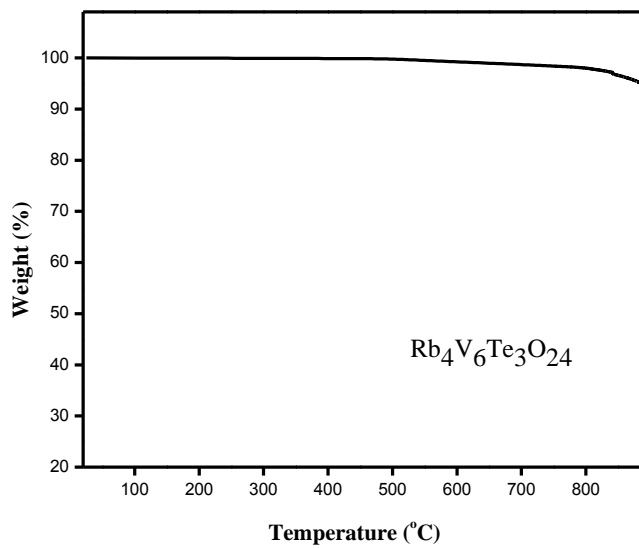
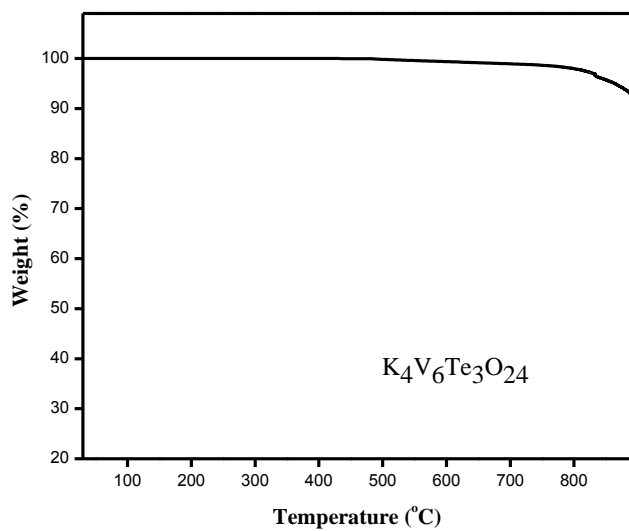
S3. Experimental and calculated powder X-ray diffraction patterns for  $\text{K}_4\text{V}_6\text{Te}_3\text{O}_{24}$



S4. Experimental and calculated powder X-ray diffraction patterns for  $\text{Rb}_4\text{V}_6\text{Te}_3\text{O}_{24}$



S5. Thermogravimetric plots for  $K_4V_6Te_3O_{24}$ ,  $Rb_4V_6Te_3O_{24}$ .



S6. Bond strain index (BSI), global instability index (GII) and bond valence data for  $K_4Te_3V_6O_{24}$  and  $Rb_4Te_3V_6O_{24}$

<b>Compound</b>		<b><math>K_4V_6Te_3O_{24}</math></b>	<b><math>Rb_4V_6Te_3O_{24}</math></b>
<b>BSI</b>		0.076	0.072
<b>GII</b>		0.146	0.141
<b>BVS</b>	<b>Te<sup>4+</sup></b>	3.80	3.80
	<b>Te<sup>6+</sup></b>	6.16	6.08
	<b>V<sup>5+</sup></b>	5.06	5.10
	<b>O(1)<sup>2-</sup></b>	2.38	2.37
	<b>O(2)<sup>2-</sup></b>	2.09	2.09
	<b>O(3)<sup>2-</sup></b>	1.89	1.92
	<b>O(4)<sup>2-</sup></b>	1.54	1.57